PROCEEDINGS OF SPIE

SPIE-The International Society for Optical Engineering

Laser Technology 2016: Progress and Applications of Lasers

Jan K. Jabczyński
Ryszard S. Romaniuk
Editors

27-30 September 2016
Jastarnia, Poland

Organized by
Military University of Technology, Warsaw (Poland)
Warsaw University of Technology (Poland)
Warsaw University (Poland)
Wrocław University of Technology (Poland)

Sponsored by
Committee on Electronics and Telecommunication, Polish Academy of Sciences
Polish Committee for Optoelectronics, Association of Polish Electrical Engineers
Photonics Society of Poland
Ministry of Science and Higher Education, Warsaw, Poland

Volume 10159
SPIE

Parametric studies on the nanosecond laser micromachining of the materials

M. Tański*[a], J. Mizeraczyk[b]
[a]Centre of Plasma and Laser Engineering, Institute of Fluid Flow Machinery, PAS, Fiszera 14, 80-231 Gdańsk, Poland; [b]Departament of Marine Electronics, Gdynia Maritime University, Morska 81-87, 91-255 Gdynia, Poland

ABSTRACT

In this paper the results of an experimental studies on nanosecond laser micromachining of selected materials are presented. Tested materials were thin plates made of aluminium, silicon, stainless steel (AISI 304) and copper. Micromachining of those materials was carried out using a solid state laser with second harmonic generation $\lambda = 532$ nm and a pulse width of $\tau = 45$ ns. The effect of laser drilling using single laser pulse and a burst of laser pulses, as well as laser cutting was studied. The influence of laser fluence on the diameter and morphology of a post ablation holes drilled with a single laser pulse was investigated. The ablation fluence threshold (F_{th}) of tested materials was experimentally determined. Also the drilling rate (average depth per single laser pulse) of holes drilled with a burst of laser pulses was determined for all tested materials. The studies of laser cutting process revealed that a groove depth increases with increasing average laser power and decreasing cutting speed. It was also found that depth of the laser cut grooves is a linear function of number of repetition of a cut. The quantitative influence of those parameters on the groove depth was investigated.

Keywords: laser micromachining, ablation, drilling, cutting

1. INTRODUCTION

Laser micromachining is a technological process with the goal of removing (ablating) small fragments of material by the means of high power laser radiation in order to form a material into a desired shape or create on its surface a spatial pattern. This technique is routinely used in the industry for micro-hole drilling, cutting, dicing and scribing in applications where high precision is required. For this reason laser micromachining features a wide range of applications in various fields such as: electronics, biology, automotive, photovoltaic, etc. [1-7].

Despite many advantages of picosecond and femtosecond lasers for micromachining nowadays nanosecond solid state lasers are still the most common and widespread type of lasers used for industrial micromachining. This is due to their high productivity, reliability and a relatively low price. However, nanosecond laser ablation is a complex process, depending on many energetic and dynamic parameters of the laser radiation, so that practical implementation of this technique may prove exceptionally difficult in various applications. For this reason experimental and theoretical attempts have been made for better understanding and optimizing a process of nanosecond laser micromachining. Although this topic has been a subject of many research the obtained results are rather limited since usually studies are focused on one particular application e.g. [8-11]. This makes it nearly impossible to make a generalization of obtained results on a wider range of applications.

In this paper the laser micromachining of common engineering materials (aluminium, silicon, stainless steel (AISI 304) and copper) was studied more extensively. This study included an investigation of blind hole drilling with a single laser pulse and a burst of laser pulses, as well as laser cutting. The effects of laser micromachining of tested materials were observed using method of optical microscopy. The results of those studies can be directly applied for parametrical optimization of the laser micromachining process in various industrial applications.

Laser Technology 2016: Progress and Applications of Lasers, edited by
Jan K. Jabczyński, Ryszard S. Romaniuk, Proc. of SPIE Vol. 10159, 101590Q

2. EXPERIMENTAL SETUP AND METHODS

The experiment was carried out using a nanosecond, Q-switched, solid state Nd:YAG laser at wavelength $\lambda = 532$ nm of the second harmonic (SHG, fundamental wavelength was $\lambda = 1064$ nm). The laser pulse width was $\tau = 45$ ns measured at the full-width at half-maximum (FWHM) of pulse intensity profile. Laser was operated in a single pulse mode, a burst mode (pulse repetition rate was f = 3 kHz) and in a continuous repetition mode (f = 6 kHz). The laser pulse energy ranged from 10 µJ to 1.3 mJ in the single pulse mode, what corresponds to the laser fluence ranging from 0.4 J/cm^2 to 42 J/cm^2. In the continuous repetition mode three values of average laser power were used 3 W, 5 W and 7 W. The laser pulse energy and laser power was measured with the Coherent LabMax-TOP powermeter equipped with J-10MT-10KHZ, J-25MT-10KHZ, J-50MT-10KHZ laser pulse energy probes and PM10V1 laser power probe.

The laser beam was focused at normal incidence to the surface of the target materials (along Z axis) using a lens with a focal length of 20 cm as it is shown in the figure 1. The beam waist was $\omega_0 = 60$ µm in diameter. The material was positioned in such a way that its surface was always in the plane of the beam waist. The displacement of the material during cutting process was realized by an Alio AI–LM–10000 XY translation stages controlled with a computer software. Maximal translation velocity of the stage in each axis was 150 mm/s.

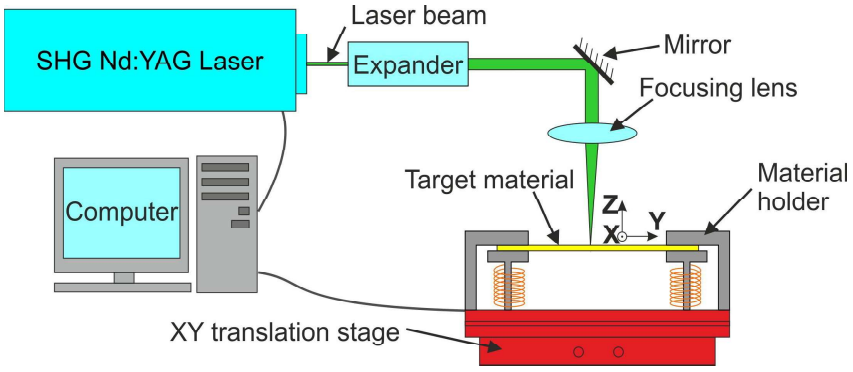

Figure 1. Experimental setup for the laser micromachining of the materials

The blind holes were drilled in the surface of the materials using two methods: single pulse drilling and percussion drilling using a burst of laser pulses. During a single pulse drilling the laser fluence was a variable parameter (the pulse energy was modified). In the percussion drilling a variable parameter was a number of pulses in burst and the laser fluence was constant. The number of pulse in burst was modified in the range from 1 to 10. In the laser cutting experiment the variable parameters were: average power of the laser beam, cutting speed and a number of repetition of a cut. The cutting speed was modified from 1 mm/s to 150 mm/s and number of repetition of a cut from 1 to 12. Both drilling and cutting procedures were carried out in ambient air in the temperature of 23˚C.

The effect of drilling and cutting of tested materials was examined using optical microscopy method. To this end Nikon Eclipse TS-100 microscope equipped with default Nikon lens ×10, ×20, ×50 and CCD camera was used. Microscopic images were used to determine the diameter of the holes drilled with a single laser pulses, as well as depth of both: percussion blind holes drilled with a burst of laser pulses and after-cut grooves. In order to measure the depth of blind holes a method of extended depth of field (EOD) was applied. In this method a set of microscopic images of hole is taken, each at different focal position. Next the computer software detects “in focus” areas in each image and merge them in a single three-dimensional map featuring the hole profile. Resulting map is analysed and the hole depth is determined. In order to determine a depth of a laser cut grooves the microscopic images showing the cross-section along the groove were taken. The range of discolouration of the groove wall indicates the penetration depth of the laser beam into the material. Thus the groove depth can be directly determined.

In the experiment four materials in the form of square plates were tested. Those materials were: aluminium (type 3003), stainless steel (AISI 304) and copper (type 110) with a thickness of 500 µm and a polycrystalline silicon plate with a thickness of 450 µm. The chemical composition of the tested materials is presented in the table 1. Before experiment surfaces of the tested materials were ultrasonically cleaned in the isopropyl alcohol and wiped dry.

Table 1. Chemical composition of tested materials

Material	Composition
Aluminium (type 3003)	Al – 98.6%, Mn – 1.2%, Cu – 0.12%
Silicon	Si > 99.99% (polycrystalline silicon)
Stainless steel (AISI 304)	Fe – 70.34%, C – 0.03%, Mn – 2%, Si – 0.75%, Cr – 18%, Ni – 8%, Mo – 0.4%, P – 0.045%, S – 0.03%
Copper (type 110)	Cu > 99.9%, trace amount of O and Ag

3. RESULTS AND DISCUSSION

3.1 Laser drilling using a single laser pulses

In the surface of each tested material a 15 measurement series of blind holes were drilled using a single laser pulses. Each series consisted of 100 holes drilled with the constant energetic parameters of the laser radiation. A variable parameter between the series was the laser fluence (the laser pulse energy was modified). The pulse energy varied from 10 µJ to 1.3 mJ what corresponded to the laser fluence ranging from 0.4 J/cm^2 to 42 J/cm^2. Drilled holes were separated by 200 µm from each other. Figure 2 shows a typical result of holes drilled in tested materials using a single laser pulses. The sequence of images in each column corresponds to the increasing value of the laser fluence for specific material.

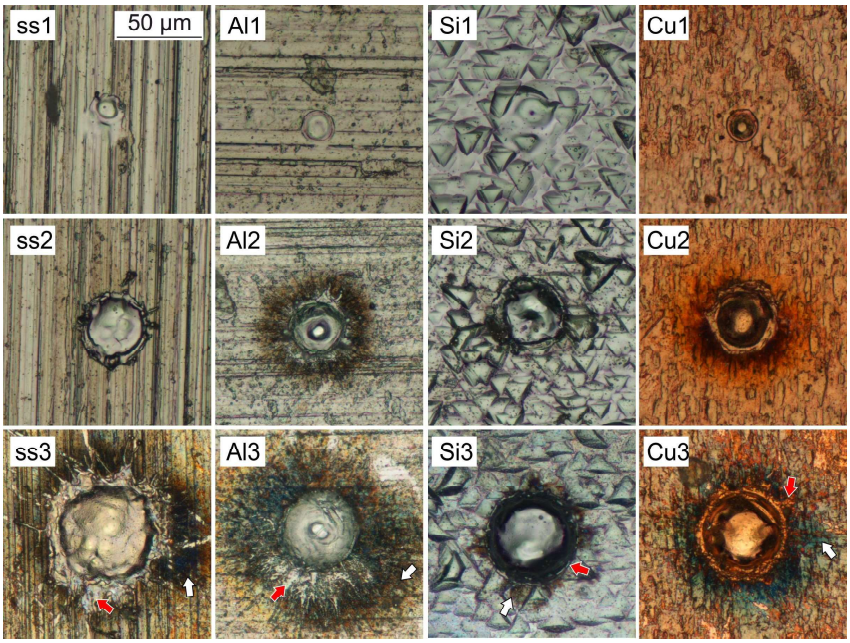

Figure 2. Microscopic images of the post ablation blind holes drilled with a single laser pulses in the surfaces of ss - stainless steel (AISI 304), Al - aluminium, Si - silicon and Cu - copper (order of columns). The sequence of images in each column corresponds to the increasing value of the laser fluence. Fluence: F_{ss1} = 1.3 J/cm^2, hole diameter D_{ss1} = 12 µm, F_{ss2} = 3 J/cm^2, D_{ss2} = 32 µm, F_{ss3} = 22.2 J/cm^2, D_{ss3} = 55 µm, F_{Al1} = 2 J/cm^2, D_{Al1} = 16 µm, F_{Al2} = 6.6 J/cm^2, D_{Al2} = 31 µm, F_{Al3} = 23.5 J/cm^2, D_{Al3} = 47 µm, F_{Si1} = 2.7 J/cm^2, D_{Si1} = 15 µm, F_{Si2} = 6.6 J/cm^2, D_{Si2} = 34 µm, F_{Si3} = 26.8 J/cm^2, D_{Si3} = 53 µm, F_{Cu1} = 3.3 J/cm^2, D_{Cu1} = 15 µm, F_{Cu2} = 8.4 J/cm^2, D_{Cu2} = 32 µm, F_{Cu3} = 23.5 J/cm^2, D_{Cu3} = 46 µm. Red arrow - spatter structures, white arrow - surface discolouration.

In the regime of nanosecond laser pulses the main mechanisms of material ablation are vaporization and ejection of the liquid phase caused by both (1) vapour pressure and by (2) phase explosion resulting from a homogeneous boiling of a liquid phase [12]. Thus during ablation caused by the nanosecond laser pulses a significant amount of liquid phase is

generated and the heat-affected zone (HAZ) is typically larger than the one formed by the pico and femtosecond laser pulses. A melted material that was not totally ejected from the irradiation region forms a spatter structures on a target surface (marked with a red arrows in the figure 2). From figure 2, length of the spatter structures increases with the laser fluence. The longest observed spatters had a length of approximately 30 µm (in the direction parallel to the material surface) and 5 µm in height. The discolouration of the surface around the irradiation region was also observed (marked with a white arrows in the figure 2). The surface discolouration is the effect of a heat conduction from the irradiation region, as well as a heat transfer from the hot ablation debris falling onto the material surface.

The diameter of the holes drilled with a single laser pulses was measured based on the microscopic images. The results are presented in the form of the plot in figure 3 showing the hole diameter as the function of laser fluence for four tested materials. The measurement points in the figure 3 were calculated as arithmetic mean diameter from 100 measurements in each series of holes. Standard deviation was marked with a vertical bars in the plot.

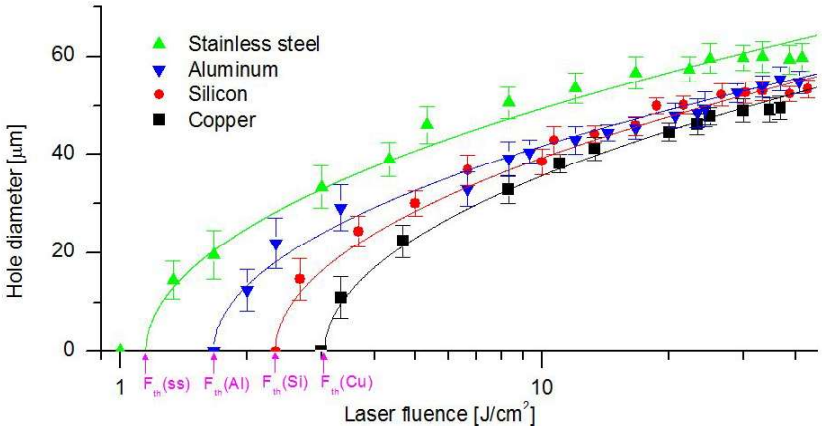

Figure 3. Relationship between the hole diameter drilled with a single laser pulses and the laser fluence for four tested materials. A curves were fitted to the measured data with equation (1).

Figure 3 shows that a significant ablation of the material starts when the laser pulses have the energy above the threshold fluence F_{th}. The diameter of the post ablation holes increases with the laser fluence. The relationship between a diameter of the hole d drilled with a single laser pulse of a Gaussian-like spatial energy distribution in respect to the laser fluence F can be expressed with the equation (1) [13,14].

$$d = \omega_0 \sqrt{2 \ln\left(\frac{F}{F_{th}}\right)}, \qquad (1)$$

where ω_0 is the beam diameter on the surface of the material. Form equation (1) it is clear that as the laser fluence decreases to the threshold value F_{th}, the diameter of the hole converges to zero. The relation described by the equation (1) was used to fit the measurement data in the plot in the figure 3 using a chi–squared method. In general the data point in the figure 3 are well fitted with the relation described by the equation (1). The slight incongruity can be observed for large values of the laser fluence (above 10 J/cm^2). This incongruity is the most likely an effect of absorption of the laser radiation by the ablation plasma. As the result less energy is transmitted to the material surface what reduce the ablation efficiency. The values of the ablation threshold determined using a fitting method can be found in the table 2. In the table 2 the reference values of ablation threshold from the literature were also provided.

From table 2 it can be seen that materials listed in the terms of increasing value of ablation threshold is as follows: stainless steel (F_{th} = 1.1 ± 0.2), aluminium (F_{th} = 1.7 ± 0.2), silicon (F_{th} = 2.3 ± 0.1) and copper (F_{th} = 3.1 ± 0.2). The values of ablation threshold of tested materials determined in this study are generally in agreement with the values from the literature. Only the ablation threshold of silicon was found to be approximately two times larger than the value obtained in [15] and [19]. The variance in the ablation threshold of silicon is probably caused by the different experimental conditions, as well as condition of the tested samples.

Table 2. Values of ablation threshold fluence of tested materials.

Material	Ablation threshold [J/cm^2]	
	This paper	Other papers
Stainless steel (AISI 304)	1.1 ± 0.2	1.0 [15]
Aluminium (type 3003)	1.7 ± 0.2	1.3 [16], 2.3 [17], 2.0 [18]
Silicon	2.3 ± 0.1	1.1 [15], 1.3 [19]
Copper (type 110)	3.1 ± 0.2	1.6 [16], 2.5 [15], 8.0 [18]

3.2 Percussion laser drilling using a burst of laser pulses

A blind holes were drilled in the surface of the tested materials with a burst of laser pulses using a percussion drilling method. In this method the subsequent laser pulses hit the material into the same spot, each laser pulse results in deepening of the hole. The time between the laser pulses was 0.33 ms (f = 3 kHz). The pulse energy of a single laser pulse was 300 µJ, after focusing onto the surface of the material it gives the laser fluence of 10 J/cm^2.

A 10 series of holes were drilled in the surface of the materials. Each series contained 10 holes drilled with the fixed values of laser radiation parameters. The variable parameters changed between the series was the number of laser pulses in burst. The number of pulses in burst ranged from 1 to 10.

The depth of the holes was measured using an extended depth of field (EOD) method with Nikon TS-100 microscope. The depth uncertainty was 1 µm. A typical example showing the cross section of the hole profile map obtained using EOD method is presented in the figure 4. In order to enhance a visual features of the profile a microscopic image of the hole was added as the map texture of hole profile. The blind hole presented in the figure 4 was drilled in the copper target with a burst of 7 laser pulses.

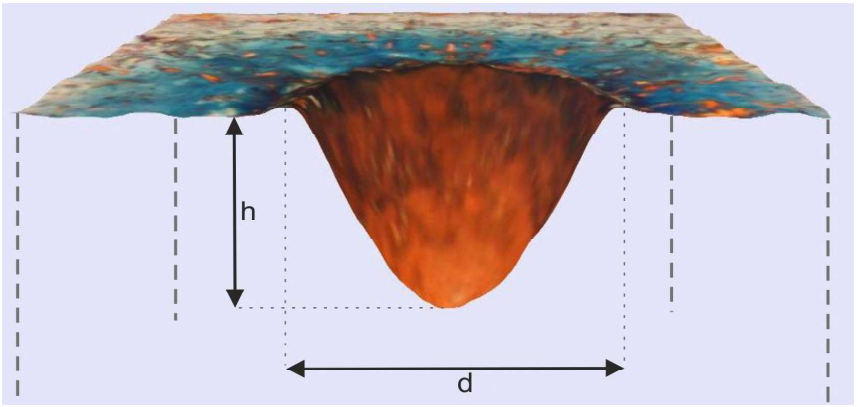

Figure 4. A Cross section of the hole profile map obtained using a EOD method. The hole was drilled using a percussion drilling method with a burst of 7 laser pulses. Pulse energy - 300 µJ, hole depth h = 28 µm, hole diameter d = 39 µm.

From the figure 4 it can be seen that the percussion-drilled hole have the cone-like shape and constrict at the bottom, this is due to the spatial distribution of energy in the used Gaussian-like laser beam. It was found that the inlet diameter of the hole is approximately constant regardless the number of pulses in burst. In the case of hole drilled in the copper target (figure 4), the inlet hole diameter was d = 39 µm. It was also found that hole depth increases with the number of pulses in burst. Figure 5 shows the influence of the number of laser pulses in burst on the depth of percussion-drilled hole. Data points in the plot correspond to the arithmetic mean value calculated for the 10 measurements in series. Vertical bars represent the standard deviation from the mean value. Using the applied method of EOD it was impossible to measure the depth of holes deeper than approximately 50 µm. This was due to the dispersion of light on the hole walls what

prevented from capturing a sharp image of the hole bottom. Moreover for deeper holes the gathering of the post ablation debris in the hole was observed what additionally obstructed the measuring method.

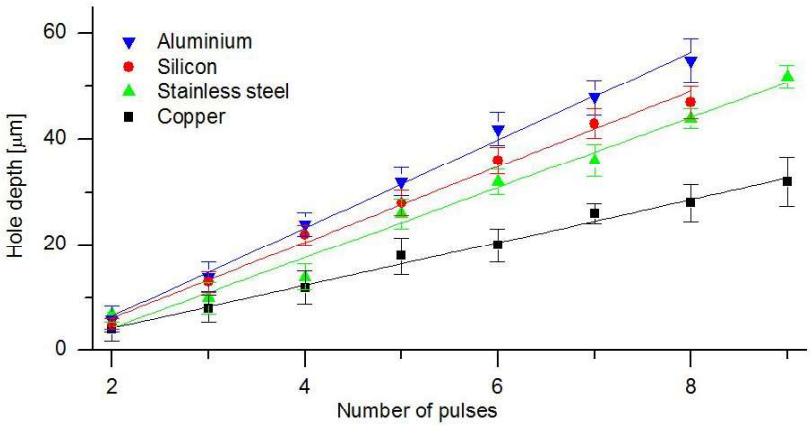

Figure 5. Depth of the percussion drilled hole as a function of number of laser pulses in burst for four tested materials. Pulse energy - 300 µJ, single pulse fluence - 10 J/cm^2, pulse repetition rate - 3 kHz.

From the figure 5, the depth of the percussion drilled hole is the linear function of number of pulses in burst for all tested materials. The slope of the solid line that fits the experimental data points gives the drilling rate (average depth per single laser pulse). The drilling rate (at fluence of 10 J/cm^2) is 8.8 µm/pulse for aluminium, 7.8 µm/pulse for silicon, 6.8 µm/pulse for stainless steel (AISI 304) and 4.0 µm/pulse for copper.

It would be intuitively expected that order of the materials listed by the decreasing drilling rate (figure 5) and by the increasing ablation threshold (figure 3) should be the same since the lower the ablation threshold the more energy of the laser pulse is used for material ablation. However results do not confirm this hypothesis. This inconsistency is most likely caused by effects related to heat transfer that takes place during nanosecond laser ablation of the materials in the liquid phase.

3.3 Laser cutting

Laser grooves were manufactured on the surface of tested materials by means of displacing a materials in XY plane under a focused laser beam. The laser was working in the continuous repetition mode (f = 6 kHz) and the experiment was performed for three values of average laser power 3 W, 5 W and 7 W (pulse energy was modified). The cutting speed was a variable parameter changed in the range from 1 mm/s to 150 mm/s.

In the figure 6 a typical microscopic images showing the cross-section along the laser cut groove made in copper plate for three values of the cutting speed are presented. The groove depth was determined based on the visible changes in the material structure caused by the laser radiation. Above the penetration depth the laser radiation caused the discolouration of the material (brown area in the figure 6). Below the penetration depth the material structure was intact (gray area). The boundary between the discoloured and non- discoloured region indicates the beam penetration depth and was marked with the red dash lines in the figure 6.

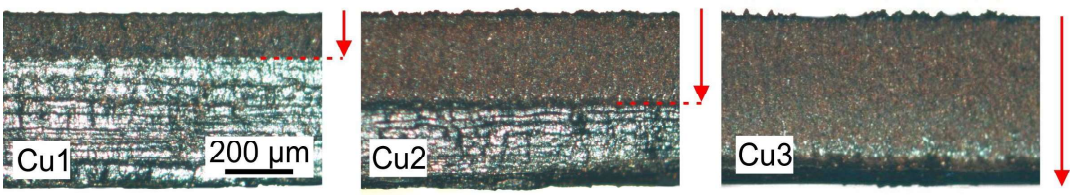

Figure 6. A Cross-section of the laser cut groove of the 500 µm thick copper plate for three values of the cutting speed. The laser beam hits the material from the top. Average beam power P = 5 W, Cu1) cutting speed V = 20 mm/s, grove depth g = 141 µm, Cu2) V = 5 mm/s, g = 275 µm, Cu3) V = 1 mm/s, g = 500 µm (plate was cut through). The red dash line indicates the beam penetration limit, a red arrow indicates the groove depth.

Plots presented in the figure 7 show the depth of the laser cut grooves as the function of cutting speed. The depth uncertainty was marked with the vertical bars in the plots. In order to simplify the identification of the measurement series data points were connected with the solid lines.

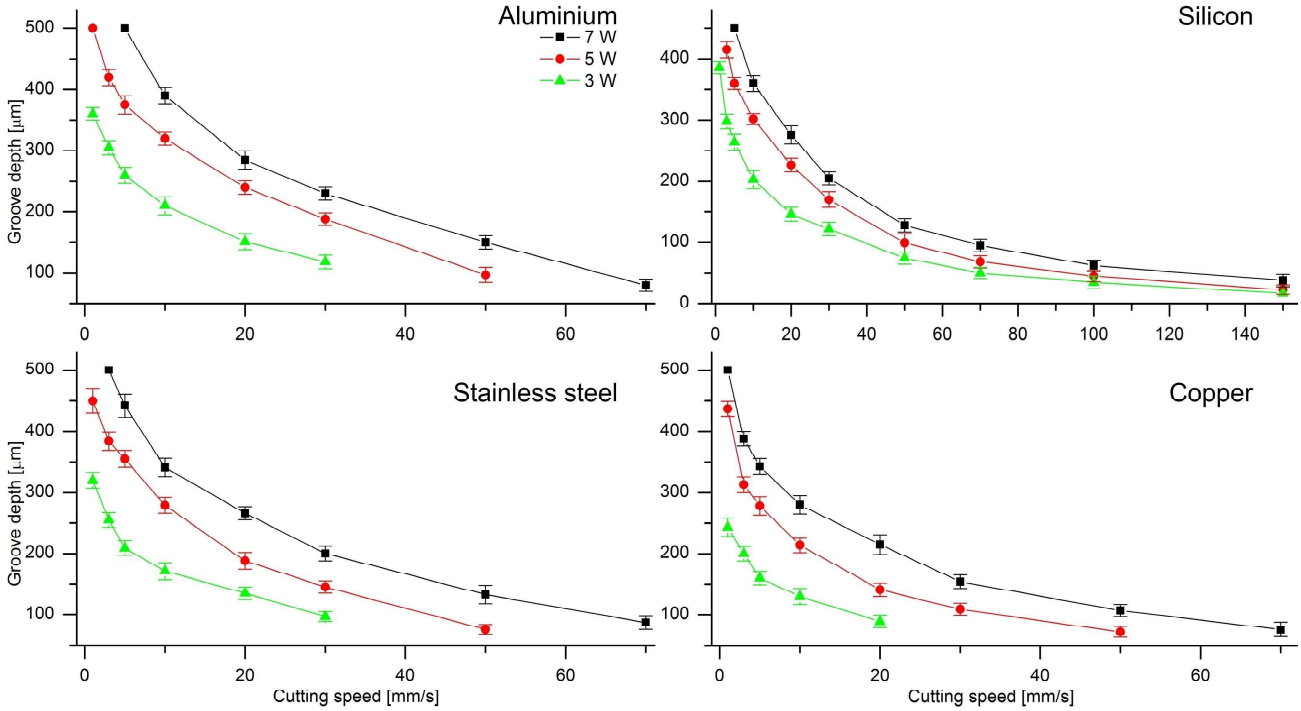

Figure 7. Depth of the laser cut grooves as the function of cutting speed for three values of the average laser power. Pulse repetition rate f = 6 kHz. Data points were connected with the solid lines.

From figure 7 it is clear that groove depth increases with increasing average laser power and decreasing cutting speed. Materials listed in order of decreasing value of the cutting efficiency (for certain value of cutting speed and beam power) is the same as an order of drilling rate of those materials (this order is as follows: aluminium, silicon, stainless steel AISI 304 and copper). This is expected since the mechanism of material ablation for laser drilling and cutting processes are similar.

The mechanism of laser ablation in the regime of nanosecond laser pulses is complicated and it involves processes like: heat diffusion, phase transition, material removal in both vapour and liquid phase as well as plasma interaction. This makes the theoretical modelling of nanosecond laser ablation truly challenging. However Black proposed a simple analytical model of laser cutting based on the energy balance [20]. In this model various simplification of the ablation process were assumed (e.g. material is exposed to continuous laser radiation and ablation takes place only via vaporization). This model allows for estimation of the groove depth g as the function of average laser power P, cutting speed v and physical parameters of the material using equation (2).

$$g = \frac{P}{v}(1-R)\left[\pi^{1/2} r \rho (c\Delta T + L)\right]^{-1}, \qquad (2)$$

where R is the material reflection coefficient, r - laser spot radius, ρ - material density, c - specific heat, ΔT - temperature difference between initial temperature of the material and the melting point, L - latent heat of vaporisation. The quantitative determination of the groove depth based on the equation (2) may be highly inaccurate due to the fact that model was derivate for the continuous laser radiation and numerous simplification of the ablation process were assumed. Nevertheless equation (2) will be used in the following qualitative analysis. For this analysis in the figure 8 grove depth made in the copper plate was presented as a function of linear density of the laser energy E_L, defined as quotient of

average beam power and cutting speed (P/v). The following analysis was done for the copper target but it can be extended over rest of tested materials.

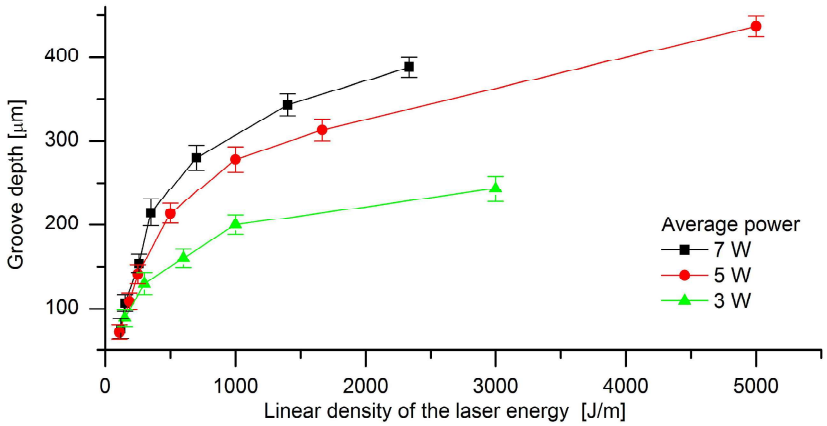

Figure 8. Depth of the laser cut grooves as the function of linear density of laser energy for copper target. Data points were connected with the solid lines.

Figure 8 shows that the depth of the laser groove increases with the linear density of the laser energy E_L, however it is not a linear relationship as expected from the equation (2). Increment of the groove depth is relatively large for small values of the linear density of the laser energy, but it is getting smaller for larger values, what corresponds to the decreasing cutting speed. It is not clear what is the reason of decrease in cutting efficiency for the larger values of linear density of the laser energy. Presumably it is cause by the hydrodynamic effects taking place in the liquid phase during material ablation using nanosecond laser pulses which were not predicted in the model proposed by Black.

Next laser grooves were manufactured in the copper target for various number of repetition of a cut. Cutting speed was a constant parameter v = 30 mm/s and number of repetition of cut was changed from 1 to 12 resulting in 7 measurement series. Each cut in a series was made "one pass on another" with a fixed parameters of the laser radiation. Laser power was a variable parameter. Plot in the figure 9 shows the depth of a laser cut groove as the function of number of repetition of a cut.

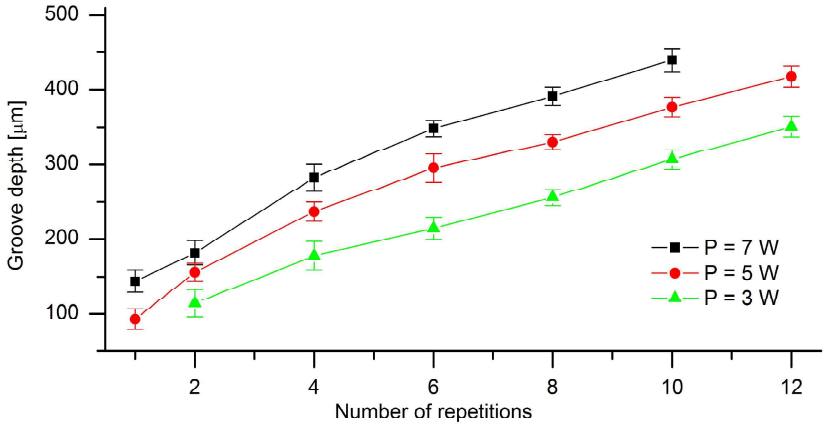

Figure 9. Depth of the laser cut grooves as the function of number of repetition of a cut. Material - copper plate. Data points were connected with the solid lines.

Figure 9 shows that the depth of the laser cut grooves is a linear function of number of repetition of a cut. That means that from a practical point of view increasing a number of repetition of a cut or proportionally increasing a laser power would result in similar increase in the groove depth. Also comparing a plots in the figure 8 and in the figure 9 it is clear

that in order to manufacture deep grooves it is more energetically favourable to repeat a cutting process multiple times with a relatively high cutting speed than performing a single cut with a low cutting speed since for low speeds cutting efficiency is significantly reduced.

4. CONCLUSIONS

Laser micromachining of plates made of aluminium, silicon, stainless steel (AISI 304) and copper using nanosecond laser pulses was studied experimentally. The effect of laser drilling using single laser pulse and a burst of laser pulses, as well as laser cutting of selected materials was investigated. Microscopic images of the post-ablation, blind holes drilled with a single laser pulse showed that the hole diameter increases with the laser fluence. The ablation threshold for all tested materials was determined. For stainless steel ablation threshold fluence was F_{th} = 1.1 J/cm^2, for aluminium F_{th} = 1.7 J/cm^2, for silicon F_{th} = 2.3 J/cm^2 and for copper F_{th} = 3.1 J/cm^2. The determined values of ablation threshold were in a reasonably good agreement with values from literature. Drilling of blind holed with a burst of laser pulses showed that hole depth increases linearly with the number of pulses in burst. The drilling rate (average depth per single laser pulse) was determined for all tested materials. Studies of the laser cutting process revealed that the depth of the laser cut groove increases with increasing average laser power and decreasing cutting speed. The quantitative influence of those parameters on the groove depth was studied and compared with the theoretical predictions of analytical model of laser cutting. It was found that groove depth is not inversely proportional to a cutting speed as it was expected. The reason of this inconsistency is unclear, presumably it is caused by the simplification of the ablation mechanism used in an analysed model. It was also found that depth of the laser cut grooves is a linear function of number of repetition of a cut.

REFERENCES

[1] Lee, J. H., Shu, D. S., Kim, J. O. and Lee Y. M., "Development of Laser Process and System for Stencil Manufacturing", Int. J. of the Korean Soc. of Precision Eng. 4, 23-29 (2003).

[2] Nowak, M. R., Atończak, A. J., Kozioł, P. E. and Abramski. K. M., "Laser prototyping of printed circuit boards", Opto-Elec. Rev. 21, 320-325 (2013).

[3] Muhammad, N., Whitehead, D., Boor, A., Oppenlander, W., Liu, Z. and Li, L., "Picosecond laser micromachining of nitinol and platinum–iridium alloy for coronary stent applications", Appl. Phys. A 106, 607-617 (2012).

[4] Schreck, S. and Zum Gahr, K. H., "Laser-assisted structuring of ceramic and steel surfaces for improving tribological properties", Appl. Sur. Sci. 247, 612-622 (2005).

[5] Chang, T. L., Chen, C. Y. and Wang, C. P., "Precise ultrafast laser micromachining in thin-film CIGS photovoltaic modules", Microelect. Eng. 110, 381-385 (2013).

[6] Schaeffer, R. D., [Fundamentals of Laser Micromachining], CRC Press, Boca Raton, 121-157 (2012).

[7] Mishra, A. and Yadava, V., "Laser Beam Micro Machining (LBMM) – A review", Opt. & Laser in Eng. 73, 89-112 (2015).

[8] Ghoreisi, M. and Nakhjavani, O. B., "Optimisation of effective factors in geometrical specifications of laser percussion drilled holes", J. Mat. Proc. Tech. 196, 303-310 (2008).

[9] Meriche, F., Neiss-Clauss, E., Kremer, R., Boudrioua, A., Dogheche, E., Fogarassy, E., Mouras, R. and Bouabellou, A., "Micro structuring of $LiNbO_3$ by using nanosecond pulsed laser ablation ", Appl. Sur. Sci. 254, 1327-1331 (2007).

[10] Sharma, A. and Yadava, V., "Modelling and optimization of cut quality during pulsed Nd:YAG laser cutting of thin Al-alloy sheet for straight profile", Opt. & Laser Tech. 44, 159-168 (2012).

[11] Hendow, S. T., Romero, R., Shakir, S. A. and Guerreiro, P. T., "Percussion drilling of metals using bursts of nanosecond pulses", Opt. Exp. 19, 10221-10231 (2011).

[12] Fishburn, J. M., Withford, M. J., Coutts, D. W. and Piper, J. A., "Study of the fluence dependent interplay between laser induced material removal mechanisms in metals: vaporization, melt displacement and melt ejection, Applied Surface Science", Appl. Sur. Sci. 252, 5182-5188 (2006).

[13] Patel, D. N., Singh, R. R. and Thareja, R. K., "Craters and nanostructures with laser ablation of metal/metal alloy in air and liquid", Appl. Sur. Sci. 288, 550-557 (2014).
[14] Liu, M. J., "Simple technique for measurements of pulsed Gaussian–beam spot sizes", Opt. Let. 7, 196-198 (1982).
[15] Martan, J., Cibulka, O. and Semmar, N., "Nanosecond pulse laser melting investigation by IR radiometry and reflection-based methods", Appl. Sur. Sci. 253, 1170-1177 (2006).
[16] Cabalin, L. M. and Laserna, J. J., "Experimental determination of laser induced breakdown thresholds of metals under nanosecond Q–switched laser operation", Spect. Acta. B 53, 723-730 (1998).
[17] Amoruso, S., Amodeo, A., Berardi, V., Bruzzese, R., Spinelli, N. and Velotta, R., "Laser produced plasmas in high fluence ablation of metallic surfaces probed by time–of–flight mass spectrometry", Appl. Sur. Sci. 96, 175-180 (1996).
[18] Vladoiu, I., Stafe, M., Negutu, C. and Popescu, I. M., "Nanopulsed ablation rate of metals dependence on the laser fluence and wavelength in atmospheric air", U.P.B. Sci. Buil. A 70, 119-126 (2008).
[19] Chen, T. C. and Darling, R. B., "Parametric studies on pulsed near ultraviolet frequency tripled Nd: YAG laser micromachining of sapphire and silicon", J. Mat. Proc. Tech. 169, 214-218 (2005).
[20] Black, I., "Laser cutting speeds for ceramic tile: a theoretical–empirical comparison", Opt. & Laser Tech. 30, 95-101 (1998).